

SEDIMENT DEPOSITION IN A SIMULATED RILL UNDER SHALLOW FLOW CONDITIONS

T. A. Cochrane, D. C. Flanagan

ABSTRACT. Eroded soil from hillslopes will deposit downslope or be transferred to waterways and deposited downstream. Understanding the interactions between shallow flows in a rill and factors such as slope, rainfall intensity, infiltration, and incoming sediment concentration are important in determining where and when sediment will be deposited. The main objectives of this study were to determine how these factors affect the deposition of non-cohesive sediment under shallow water flow in a rill and to test whether the β turbulence parameter in the WEPP model deposition equation was adequately represented for those conditions. An experimental laboratory hydraulic flume under rainfall simulators was used to study sediment deposition in a 25 cm wide by 3.6 m long rill. A laser scanner was used to quantify deposition after each experiment, and sediment samples were taken from the flume outlet to quantify sediment transport. The experiments were conducted using silica sand, glass beads, and artificial plastic/glass aggregates. Combinations of different flow rates, rainfall intensities, and sediment feed rates were studied for each sediment type at slopes varying from 1% to 5%. The interaction of rainfall intensity and flow depths had a more significant effect on deposition of particles of low specific gravity and under greater interrill sediment contributions; however, this was not true for denser sand particles. Sediment deposition in the rill was less under no rainfall and high-intensity rainfall than under medium-intensity rainfall. The effect of infiltration on sediment deposition under high-intensity rainfall was related to the slope steepness. At slopes greater than 3%, less deposition was observed under saturated conditions than under unsaturated conditions. The opposite was true for slopes less than 3%. Modeling deposition based on measured deposition rates of the non-cohesive sediment showed that the β turbulence factor for the particle and flow conditions in these experiments could be 10 or more times less than the 0.5 value currently used in the WEPP deposition equation.

Keywords. Rainfall turbulence, Rill, Sediment deposition, Soil erosion mechanics, WEPP.

Soil erosion by water is a complex mechanism that depends on various land use, weather, hydrologic, topographic, and soil properties. The combination of these factors dictates the rates at which sediment detachment, transport, and deposition occur. Although there has been much study of many aspects of soil erosion, the overall picture is not complete. One area requiring further study is the effect of rainfall, infiltration, and sediment type on sediment deposition in concentrated flow in a rill with shallow water flow depths. This is especially important for parameterization of deposition equations used in physically based erosion models, such as the Water Erosion Prediction Project (WEPP) developed by the USDA (Flanagan and Nearing, 1995). Of particular interest in this study were the

erosion equations used in WEPP for sediment deposition in a rill (Foster et al., 1995):

$$\begin{aligned}\frac{dG}{dx} &= D_r + q_s \\ D_r &= \alpha(T_c - G) \\ \alpha &= \frac{\beta V_s}{q}\end{aligned}\quad (1)$$

where G is the sediment load per unit width ($\text{ML}^{-1} \text{T}^{-1}$), x is the distance along the channel (L), D_r is the net deposition rate in rills ($\text{ML}^{-2} \text{T}^{-1}$), q_s is the lateral sediment inflow from adjacent contributing broad shallow flow areas ($\text{ML}^{-2} \text{T}^{-1}$), T_c is the transport capacity ($\text{ML}^{-1} \text{T}^{-1}$), and α is a first-order reaction coefficient (L^{-1}). The α coefficient is computed for a single particle size distribution (Foster, 1982) with the following parameters: V_s is the effective particle fall velocity (LT^{-1}), q is the flow rate per unit rill channel width ($\text{L}^2 \text{T}^{-1}$), and β is a dimensionless turbulence parameter.

The β constant is a catchall parameter that includes the turbulence of the rainfall and is theoretically bounded from zero for shallow flows and high turbulence to one for deep flows and low turbulence. β is set to 0.5 for shallow flow under rainfall in a rill in the WEPP model, but this value could potentially be improved by taking into account differences in turbulence induced by varying rainfall intensities and flow depths. The experiments in this study were

Submitted for review in January 2005 as manuscript number SW 5687; approved for publication by the Soil & Water Division of ASABE in June 2006.

The authors are **Thomas A. Cochrane, ASABE Member Engineer**, Agricultural Engineer, Natural Resources Engineering, Department of Civil Engineering, University of Canterbury, Christchurch, New Zealand, and former Graduate Research Assistant, Department of Agricultural and Biological Engineering, Purdue University, W. Lafayette, Indiana; and **Dennis C. Flanagan, ASABE Member Engineer**, Agricultural Engineer, USDA-ARS National Soil Erosion Research Laboratory, West Lafayette, Indiana. **Corresponding author:** Dennis C. Flanagan, USDA-ARS National Soil Erosion Research Laboratory, 275 S. Russell St., W. Lafayette, IN 47907-2077; phone: 765-494-7748; fax: 765-494-5948; e-mail: flanagan@purdue.edu.

designed to help in the understanding of the turbulent effects of rainfall intensity and flow depth on deposition of sediments and therefore to improve the accuracy of this parameter.

Moss and Green (1983) conducted experiments indicating that transport rates peak when raindrops impact flows that are between two and three drop diameters deep. It was also found that transport rates tend to vary linearly with flow velocity and that rainfall does not affect sediment transport for slopes greater than 9%, probably because of the high flow velocity at those slope gradients (Moss et al., 1979). In a study performed by Schmidt (1991), the direct impact of rainfall on sediment transport decreased with slope length because flow depth increased downslope. Some studies seem to indicate a definite relationship between rainfall intensity, slope, and sediment transport. These relationships incorporate other effects, such as flow velocity varying with rainfall intensity, but they do not account for flow depth. As Kinnell (1991) stated, the results of many of these experiments may have been misinterpreted because the effects of flow depth on erosion by rain-impacted flow were ignored. Kinnell (1991) verifies the work done by Moss and Green (1983) by stating that flow depth has a significant influence on the transport of particles when flow depths are less than three drop diameters. He also proposes an analytical theory for the transport of particles by raindrop-induced flow transport (RIFT) to examine the effects of rain, flow, and particle characteristics on the movement of soil material in overland flow. The term raindrop-induced flow transport (RIFT, Kinnell, 1988) was introduced to describe the effects of rainfall impacts that induce flow to transport particles, which the flow would not be able to do on its own.

Beuselinck et al. (1999) and Beuselinck et al. (2002) reported results of laboratory studies of sediment deposition from overland flow under no rainfall and rainfall conditions, respectively. In these experiments, sediment-laden water was introduced at the top of a 2.6 m long by 11.7 cm wide non-infiltrating flume, and in the second study subjected to a rainfall rate of 45 mm h⁻¹. Silty material was used, with about 90% of the sediment less than 63 μm in size. These studies provided very valuable information on sediment transport and deposition for fine materials under a relatively low-intensity rainfall. The experiments conducted by Moss and Green (1983), Moss (1988), Kinnell (1991), and Beuselinck et al. (1999, 2002) made significant contributions to the understanding of the influences of rainfall on shallow flow; however, they were largely directed to simulation conditions of overland flow. Although the results are still valuable for the study of shallow flow in rills, actual experiments on the effects of channelized flow on sediment transport are needed under a range of rainfall and inflow sediment rates.

This article reports on a series of experiments in a hydraulic flume specially designed to quantify the interactions between flow depth, rainfall intensity, sediment type, and other factors on the deposition of non-cohesive sediment in a shallow concentrated flow rill. The objectives of the study were: (1) to determine if rainfall intensity, infiltration rate, and incoming sediment concentration had a significant effect on the deposition of non-cohesive sediment under shallow water flow in a rill, and (2) to test whether the β turbulence parameter in the WEPP deposition equation was adequately represented for non-cohesive sediment.

MATERIALS AND METHODS

EXPERIMENTAL SETUP

A hydraulic flume was designed to simulate conditions in an agricultural rill. The experimental setup included a 3.6 m long by 0.25 m wide flume with sediment feeders at the top and sides of the rill, rainfall simulators, and a laser micro-topography scanner. The setup was named the rill simulator (fig. 1) and was designed to study the effects of slope, rill width, sediment input from the top and sides, infiltration rate, sediment type, flow depth, and rainfall intensity on deposition in a rectangular rill. The rill slope was changed using a manual crank, and the rill width was set to 25 cm for all experiments to simulate agricultural rills. Rotating sediment feeders delivered sediment to the top and sides of the rill. Water inflow was mainly delivered to the top of the rill, but about 5% of the water inflow was delivered to the sides of the rill, resulting in wet sediment being introduced to the rill from the top and sides. The water inflow rate to the rill was controlled by a set of gauges and pumps, and infiltration rates were controlled by numerous hoses that drained the bottom of the rill and were connected to a single adjustable flowmeter. Rainfall intensity was set for each experiment by using a programmable laboratory rainfall simulator (Foster et al., 1982), and a system of plastic covers limited rainfall to the surface area of the rill. The laser scanner (Flanagan et al., 1995) was used to measure the surface

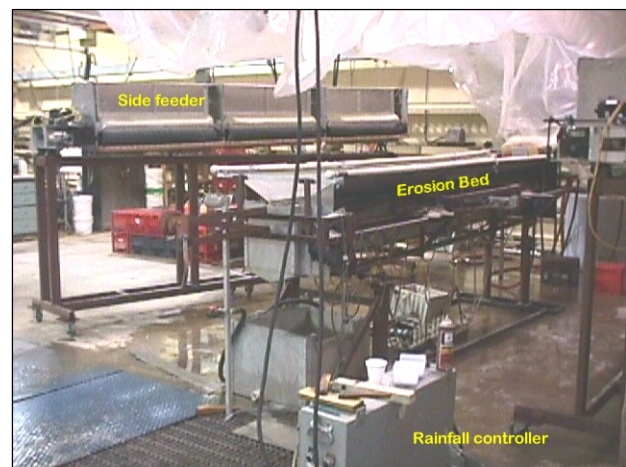


Figure 1. Rill simulator used to conduct experiments of deposition in rills.

Table 1. Rill simulator experiments using sand, glass beads, and plastic/glass aggregates under different rainfall intensities, infiltration rates, flow rates, and sediment feed rates.

Experiment Group	Sediment Type	Slope (%)	Rainfall / Infiltration (mm h ⁻¹)	Water Flow Rates (L min ⁻¹)	Sediment Feed Rates		No. of Different Runs	Total Replications per Run ^[a]
					Top (g s ⁻¹)	Side (g s ⁻¹)		
A	Sand	1	0 / 0	22.7 30.3	0	0	18	2
			80 / 80		5.3			
			130 / 130		10.77			
B	Sand	1	80 / 0	22.7 30.3	5.3	0	8	2
			130 / 0		10.77			
C	Sand	1	100 / 100 170 / 170	53 58	0	100	4	3
D	Sand	2	170 / 170 170 / 0	58	0	100	8	1 ^[b]
		3						
		4						
		5						
E	Sand	5	0 / 0	45 60	5.3	100	10	5 (rain = inf) 2 (inf = 0)
			80 / 80					
			160 / 160					
			80 / 0					
			160 / 0					
F	Glass beads	2	0 / 0	45	5.3	100	9	5
			80 / 80			45		
			160 / 160			30		
G	Glass beads	2	80 / 0 160 / 0	45	5.3	30	2	2
H	Aggregates	2	0 / 0	20 30	4.74	13.9	6	5
			80 / 80					
			160 / 160					
I	Aggregates	2	0 / 0 80 / 80 160 / 160	20 30	4.74	34.4	6	5

^[a] Represents the number of repetitions for each different run; not all repetitions greater than 2 were used as some were discarded due to errors identified during or after the run.

^[b] Only one repetition was made because this was only an initial test run for different slopes.

of the sediment bed before and after each experimental run and obtain a digital image and measurement of the deposition and detachment that had occurred as a result of the experimental treatment. The vertical resolution of the scanner is under 0.5 mm, and the horizontal resolution was set to 1 mm along the length of the rill and 5 mm along the cross-section.

Nine groups of experiments were conducted with a variety of rainfall intensities, infiltration rates, water flow rates, sediment types, and sediment feed rates to study the complex interactions between these factors (table 1). Experiment groups A through D were a series of experimental runs to test the erosional and depositional characteristics of the rill simulator. In experiment group D, only one repetition was conducted at each of four slopes because the purpose of the test runs was to identify slopes in which sand was in a depositional regime. For experiments E through I, slopes, water inflow rates, and sediment feed rate conditions were selected accordingly to obtain shallow flows and to reach a depositional stage for the specific sediment being studied under 0, 80, and 160 mm h⁻¹ rainfall intensities. Experiments in groups E and G with 80 and 160 mm h⁻¹ of rainfall and zero infiltration were conducted to study deposition under saturated soil conditions utilizing silica sand and glass beads.

The sediment materials varied in size, density, and fall velocity (table 2 and fig. 2). Specific gravity of the sand and glass beads was 2.50 to 2.65, but the plastic/glass aggregates were designed to have a specific gravity of only 1.25. Experimental fall velocities were measured using a Griffith tube (Hairsine and McTainsh, 1986). Calculated fall velocities

are not as reliable as measured fall velocities because calculations are based on an average shape factor; therefore, measured fall velocities were used for the modeling. The sand was a fine crystal silica Ottawa foundry sand from the U.S. Silica Company (0.330 mm). The glass beads were standard sandblasting abrasive spherical glass beads of U.S. sieve size number 70/140. The plastic/glass aggregate particles were created by impregnating standard spherical 3 mm polyethylene resin beads with the 0.15 mm glass beads. This was done by baking the plastic beads in a tray filled with the glass beads until the plastic softened and the glass beads became impregnated into the plastic beads. The silica sand and the glass beads erode in a similar way as natural sand. The plastic/glass aggregates erode similarly to a Cincinnati series soil, as demonstrated by conducting an experiment where the plastic/glass aggregates were well-mixed with this soil then subjected to various levels of inflowing water. Figure 3 shows that erosion rates were highly correlated between the plastic/glass aggregates and the Cincinnati series soil at 10% slope

Table 2. Physical properties of sediment used in experiments.

Sediment Type	Specific Gravity	Average Diameter (mm)	Fall Velocity ^[a]	
			Measured (m s ⁻¹)	Calculated (m s ⁻¹)
Silica sand	2.65	0.330	0.0557	0.0550
Glass beads	2.50	0.150	0.0211	0.0184
Aggregates	1.25	3.175	0.0986	0.1480

^[a] The fall velocity was calculated experimentally using the Griffith tube (Hairsine and McTainsh, 1986).

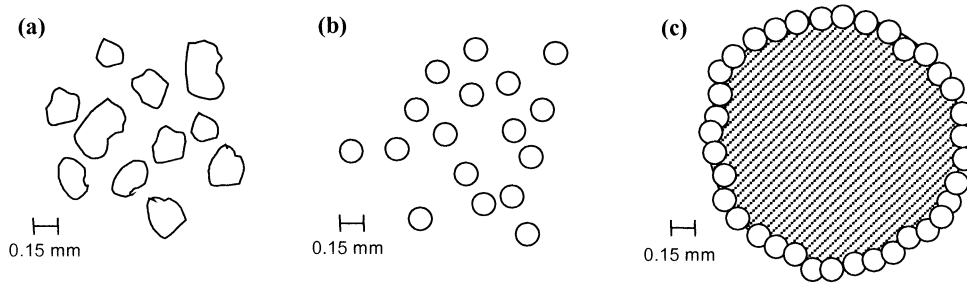


Figure 2. Schematic cross-section drawings of (a) sand, (b) glass beads, and (c) plastic/glass aggregates.

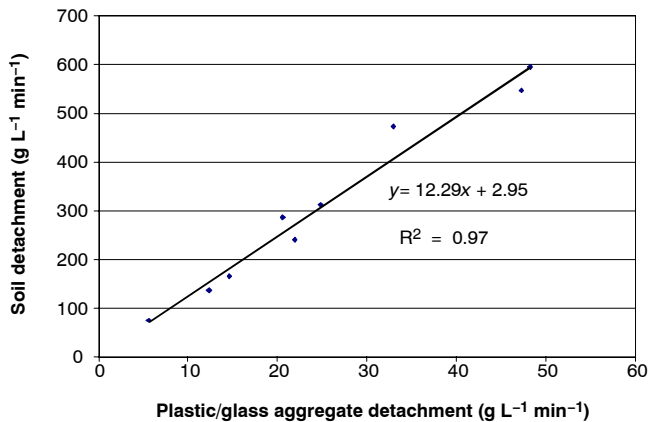


Figure 3. Detachment of plastic/glass aggregates when mixed with Cincinnati series soil on a 10% slope erodible rill flume.

at nine different water flow rates. The beads (mixed in to comprise 5% of the in-situ soil) were detached and transported at about a constant 8% of the total sediment load (fig. 3). With this material, which erodes similarly to a natural soil, it was therefore possible to study the differences in the effect of sediment size and density on deposition as influenced by rainfall intensity and flow depth.

Two types of measurements were obtained: sediment leaving the bed, and sediment being deposited on the bed. Sediment leaving the bed was measured by collecting outflow samples every minute during the 10 min runs. Sediment deposition on the bed was measured by taking

topographic laser scans before and after each experimental run. From these scans, deposition quantities in control volumes along the rill for each experiment were calculated from the difference between the initial and final laser scans (Cochrane and Flanagan, 1997). When rainfall was not present, the laser scanner could remain on top of the rill and initial and final scans would match perfectly. When rainfall was present, the laser scanner had to be moved between the initial and final scans. In order to increase the matching of the initial and final scan, thin metal strips were placed across the rill at the location where the longitudinal scans would begin and end. These strips acted as a guide to setting up the laser scanner in the correct position. Even with this extra measure, small dislocation errors (a few millimeters) occurred in the x , y , and z (height) dimensions.

A computer program was written to correct the errors by matching the location of the scanned metal strips in both the initial and final scan. Matches were done line scan by line scan, and a new data set was created for the final scan (fig. 4). The scan area for these sets of experiments was 6744.5 cm², and the total rill surface was 8500 cm² (fig. 4 dotted line). In other words, the scan covered around 80% of the rill surface area, as compared to 57% for our previous detachment experiments using the same scanning method (Cochrane and Flanagan, 1997). For this example (fig. 4), deposition and detachment amounts were calculated for ten equal-sized intervals of the scan.

DEPOSITION AND SEDIMENT TRANSPORT MODELING

The deposition in a rill was modeled by using the WEPP deposition equations presented earlier. These equations were

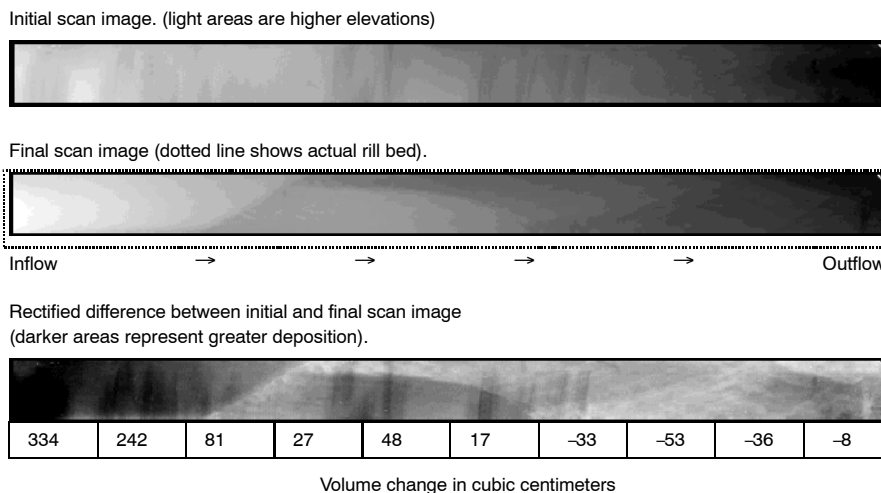


Figure 4. Example of deposition study scan images (experiment group A, rep. 1, rain = 80 mm h⁻¹, inflow = 22.7 L min⁻¹, and feed rate = 10.77 g s⁻¹).

solved using a finite difference approach, which allows the estimation of deposition down the rill. Deposition in the rill, as measured by the laser scans or the difference between sediment input and output, was dependent on the sediment flowing in from the sediment feeders (G_{in}), the sediment fall velocity (V_{fall}), the flow rate (q), the turbulence factor (β), and the transport capacity in the rill (T_c). The turbulence factor (β) can be estimated in a similar way using the equations shown below together with measured values for the other parameters.

$$G_{out} = G_{in} + L_t \cdot \left(\frac{\beta \cdot V_{fall}}{q} \right) \cdot (T_c - G_{in}) \quad (2)$$

$$\beta = \frac{D_r \cdot q}{V_{fall} (T_c - G_{in})} \quad (3)$$

$$D_r = (-1) \left(\frac{G_{acc}}{L_t} \right) \quad (4)$$

$$G_{acc} = G_{in} - G_{out} \quad (5)$$

where G_{out} and G_{in} are the sediment load going in and out of interval ($\text{kg m}^{-1} \text{s}^{-1}$), G_{acc} is the accumulation rate ($\text{kg m}^{-1} \text{s}^{-1}$), D_r is the net detachment rate ($\text{kg m}^{-2} \text{s}^{-1}$), L_t is the distance downslope or length of the rill (m), β is the dimensionless turbulence factor, V_{fall} is the effective particle fall velocity (m s^{-1}), q is the flow rate per unit channel width ($\text{m}^2 \text{s}^{-1}$), and T_c is the calculated transport capacity ($\text{kg m}^{-1} \text{s}^{-1}$). As mentioned earlier, the β factor is used to adjust the prediction for greater turbulence induced by a rainfall intensity and flow depth relationship, which may also be linked to particle size or density.

The transport capacity of flow (T_c) is an important term that is used in determining the maximum allowable sediment in the flow for the given hydraulic conditions. There exist numerous sediment transport equations to estimate this value, but only a few are used for agricultural erosion prediction because of the shallow flows and low flow rates. Alonso et al. (1981) compared sediment predictions of nine different transport formulas to measurements of flume and field data. They concluded that the Yalin (1963), Yang

(1973), and Laursen (1958) formulas give the best predictions for all flows, but the Yalin formula is more appropriate for shallow flows with sands, silts, and lightweight materials. This equation has been analyzed by many, including Foster and Meyer (1972), and based on its assumptions, derivation, and experiments, it seems to work well for predicting sediment transport in shallow flows. Subsequently, this equation was incorporated into WEPP and is used to determine the transport capacity of all sediments being modeled. The Yalin equation (Yalin, 1963) is represented by the following set of equations:

$$P = \left(\frac{W_s}{S_g \rho_w d V_*} \right) = 0.635 \delta \left[1 - \left(\frac{1}{\sigma} \right) \text{Ln}(1 + \sigma) \right]$$

$$\sigma = 2.45 S_g^{0.4} Y_{CR}^{0.5} \cdot \delta$$

$$\delta = \left(\frac{Y}{Y_{CR}} \right) - 1 \quad \text{when } Y < Y_{CR}, \delta = 0$$

$$Y = \frac{V_*^2}{(g_s - 1)gd}$$

$$V_* = (gR_f s)^{\frac{1}{2}} = \left(\frac{\tau_{cs}}{\rho_w} \right)^{\frac{1}{2}} \quad (6)$$

where P is a nondimensional sediment transport capacity, W_s is the transport capacity ($\text{ML}^{-1} \text{T}^{-1}$, T_c for uniform sediment), S_g is the particle specific gravity, ρ_w is the mass density of water (ML^{-3}), d is the diameter (L), V_* is the shear velocity (LT^{-1}), Y is a function of shear velocity and particle diameter, Y_{CR} is the ordinate from the Shields diagram (Shields, 1936), g is the acceleration due to gravity (LT^{-2}), R_f is the hydraulic radius (L), s is the slope of the energy grade line, and τ_{cs} is the shear stress acting on the soil ($\text{MT}^{-2} \text{L}^{-1}$). Modifications to the Yalin equation have been made by Foster (1982) to consider mixtures consisting of particles of varying sizes and densities and these have been included in WEPP and were used in the determination of transport capacity for these studies.

RESULTS AND DISCUSSION

EXPERIMENTS WITH SAND

For conditions when rainfall intensity was equal to infiltration rate, there was no significant effect (ANOVA and T-tests with $\alpha = 0.05$) of rainfall intensity on the deposition of sand, as shown in figure 5 for experiment group E. The deposition of sand for experiments A, B, C, D, and E (table 1) was mainly influenced by slope, water inflow, sediment feed rate, and infiltration (saturated vs. unsaturated conditions, which are presented later in this article). Although average values showed slight increases in deposition under the 80 mm h^{-1} rainfall intensity, there were no significant effects according to comparative T-tests ($\alpha = 0.05$) of rainfall intensity on sediment discharge. Meandering of flow was not observed under rainfall; however, meandering was observed in the rill with no rainfall.

Meyer et al. (1983) obtained comparable results for similar conditions of flow rates, rainfalls, and sand size and

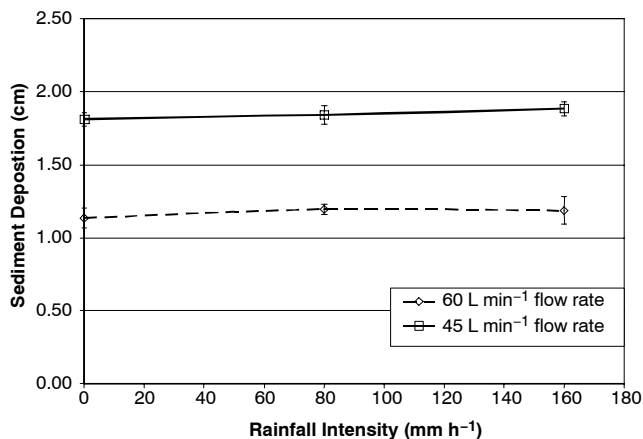


Figure 5. Deposition of sand at 0, 80, and 160 mm h^{-1} rainfall intensities and at 60 and 45 L min^{-1} flow rate for experiment group E. Error bars show one standard deviation for repetitions.

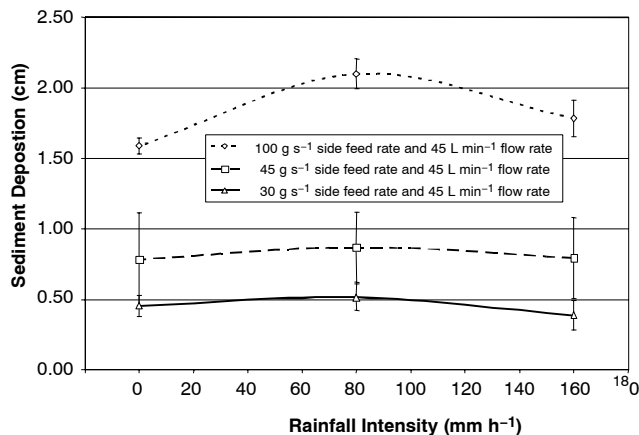


Figure 6. Deposition of glass beads (experiment group F) for three rainfall intensities with infiltration, sediment side feed rates at 2% slope, and 45 L min⁻¹ water inflow rates.

suggested that these conditions resulted in a transition phase in which rainfall intensity did not have an effect on sediment transport. Another explanation stems from visual observations that most of the sediment moved as bedload transport caused by the density of the particles and thus may not be as influenced by rainfall-induced turbulence. Foster (1982) mentions that the deposition equation could possibly be ignored for bedload transport, but may be significant for the transport and deposition of fine particles. Glass beads and plastic/glass aggregates were subsequently used to simulate uniform finer and less dense sediment under different flow conditions.

EXPERIMENTS WITH GLASS BEADS AND AGGREGATES

Experiments conducted with glass beads and plastic/glass aggregates showed that rainfall-induced turbulence had an impact on deposition. The level of this impact was dependent on whether the rill was in a high-deposition regime or a low-deposition regime. A high-deposition regime was achieved by having a larger interrill sediment contribution from the sides of the rill. Statistical T-tests ($\alpha = 0.05$) showed that for fine glass beads, rainfall of 160 and 80 mm h⁻¹ intensities caused significantly greater deposition than no rainfall under high deposition rates (100 g s⁻¹ side feed rate), and 80 mm h⁻¹ rainfall caused greater deposition than 160 mm h⁻¹ rainfall (fig. 6). Rainfall did not influence deposition of fine glass beads when the rill was in a low-deposition regime. The deposition of low-density plastic/glass aggregates was influenced by rainfall intensity at shallow flow depths (fig. 7). Experiments conducted with the high sediment feed rate (34.4 g s⁻¹) were under a depositional regime, and experiments conducted with the lesser sediment feed rate (13.9 g s⁻¹) were under a detachment regime (i.e., negative sediment deposition).

Statistical T-tests ($\alpha = 0.05$) show that within the depositional regime (fig. 7), the effect of rainfall intensity on

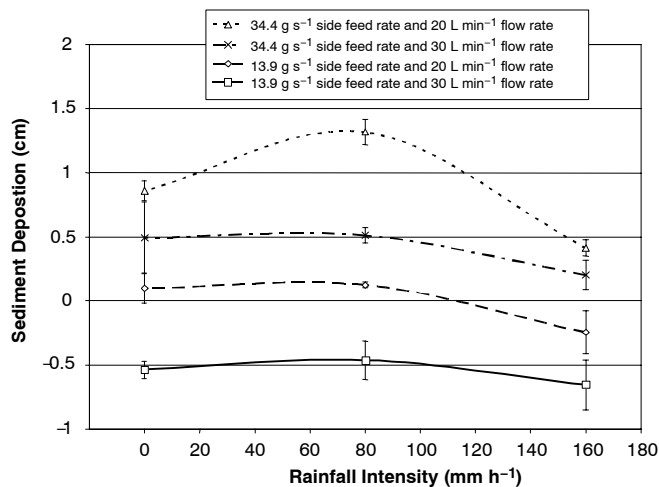


Figure 7. Deposition/detachment changes with rainfall intensity for plastic/glass aggregates (experiment groups H and I). Error bars show one standard deviation range for repetitions.

sediment transport and therefore deposition is significant for experiments with the highest sediment feed rate. For low-density particles such as the plastic/glass aggregates, no rainfall and high-intensity rainfall diminish deposition, while deposition is greater at medium-intensity rainfall. This effect is also seen in the detachment regime, but it is more pronounced in the depositional regime. Additionally, shallower flow depths (at 20 L min⁻¹ flow rate) show a greater deposition at medium-intensity rainfall, relative to no rainfall and high-intensity rainfall, than greater flow depths (at 30 L min⁻¹ flow rate). A possible explanation for this could be the fact that meandering and concentration of water flow were observed during the deposition study when rainfall was not present. This meandering could have decreased the deposition by concentrating the water flow depth and increasing the transport capacity (fig. 8).

Rainfall had a definite effect on the surface of the bed. When either the medium or high rainfall intensity was applied to the flow, the bed of the rill maintained a uniformly flat surface. Meandering of flow and formation of bed forms were greatly reduced and in most cases totally eliminated. Deposition areas were still present, but visual determination of these areas was difficult and could only be accounted for with laser scans. The high-intensity rainfall is thought to have increased flow turbulence, thus limiting deposition.

INFILTRATION EFFECTS

The influence of infiltration on deposition was studied in experiments D and E, as well as in the comparisons of experiments A with B and F with G. In these cases, deposition results from rainfall applied to a saturated (non-infiltrating) bed were compared to rainfall applied to an unsaturated (infiltrating) bed. Unsaturated conditions in the soil were represented by physically setting the infiltration rate equal to the



Figure 8. Image of final bed surface of an experiment run using sand at 2% slope without rainfall showing bed formations as a result of meandering of flow. Light areas show lower elevations and dark areas show higher elevations.

Table 3. Influences of infiltration on output and accumulation of sand at different slopes (results from experiment group E and comparisons of experiment groups A with B).

Rainfall (mm)	Flow Rate (L min ⁻¹)	Saturated Bed (no infiltration)		Unsaturated Bed (infiltration = rainfall)		Percent Difference Between Saturated and Unsaturated Beds	
		$G_{out}^{[a]}$ (kg m ⁻¹ s ⁻¹)	$G_{in} - G_{out}^{[b]}$ (kg m ⁻¹ s ⁻¹)	G_{out} (kg m ⁻¹ s ⁻¹)	$G_{in} - G_{out}$ (kg m ⁻¹ s ⁻¹)	G_{out} (%)	$G_{in} - G_{out}$ (%)
Experiment group E at 5% slope and 105.3 g s ⁻¹ total sediment feed rate							
160	45	0.236	0.178	0.236	0.178	0.0	0.0
80	45	0.234	0.181	0.233	0.181	0.0	0.0
160	60	0.340	0.075	0.309	0.105	10.0	-28.6
80	60	0.317	0.098	0.299	0.115	6.0	-14.8
Experiment groups A and B at 1% slope and 5.3 g s ⁻¹ total sediment feed rate							
80	22.7	0.00134	0.0195	0.00432	0.0165	-69.0	18.0
80	30.3	0.00318	0.0177	0.00416	0.0167	-23.4	5.8
130	22.7	0.00359	0.0173	0.00365	0.0172	-1.6	0.3
130	30.3	0.00376	0.0171	0.00740	0.0135	-49.2	27.0
Experiment groups A and B at 1% slope and 10.77 g s ⁻¹ total sediment feed rate							
80	22.7	0.00106	0.0413	0.00456	0.0378	-76.8	9.2
80	30.3	0.00382	0.0386	0.00650	0.0359	-41.3	7.5
130	22.7	0.00283	0.0396	0.00408	0.0383	-30.7	3.3
130	30.3	0.00300	0.0394	0.00513	0.0373	-41.5	5.7

[a] G_{out} = measured sediment output.

[b] $G_{in} - G_{out}$ = sediment accumulated.

rainfall intensity. Although under saturated conditions it was expected that the additional rain water and possible turbulence would increase the transport capacity and diminish the deposition, results show that this effect is dependent on slope.

Table 3 shows the influence of rainfall on a saturated bed as compared to unsaturated sand at 5% and 1% slope. Results for the 5% slope experiments (group E) show that saturated conditions had less sediment deposition (sediment accumulated) than unsaturated conditions. However, for the 1% slope experiments (groups A and B), the opposite was true. Although the data set is limited, it is interesting to note that for experiment group E the difference between saturated conditions and unsaturated conditions was only visible at the greater flow rate, although this is not obvious for the other experiments.

The results from experiment group D further show that there was a relationship between the effect of infiltration and the slope. In figure 9, one can see that for slopes greater than 3%, saturated conditions increase the transport capacity and diminish the deposition compared to unsaturated conditions; however, when the slope is below 3% deposition is greater than in unsaturated conditions. This observation is corroborated by experiments F and G using a flow rate of 45 L min⁻¹, which show that sediment deposition under rainfall is lower in unsaturated conditions at a slope of 2% (fig. 10). The data set presented here was limited and further experiments are required to establish better relationships between deposition and saturated or unsaturated conditions.

SEDIMENT TRANSPORT AND DEPOSITION MODELING

Results of experiments conducted in this study showed that calculated sediment transport capacity (T_c) using the modified Yalin equation matched measured sediment output for experiments involving sand and experiments with plastic/glass aggregates at high sediment feed rates (experiment groups A through E and I in table 1, and fig. 11). These results indicate that the Yalin equation (WEPP) works well in estimating values for T_c for both sand and plastic/glass aggregates. For the experiments with artificial aggregates

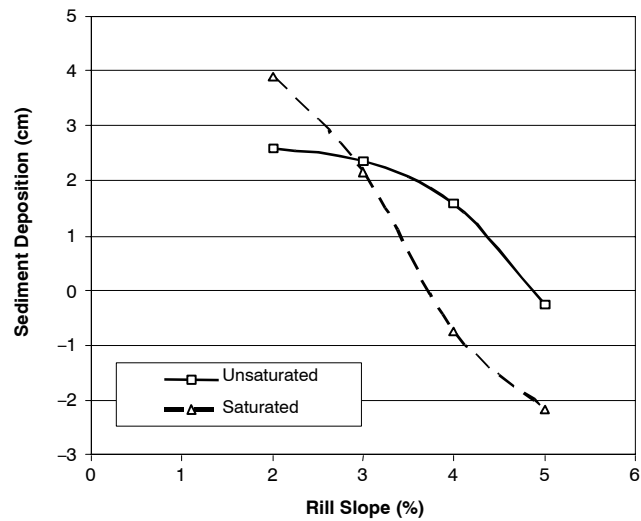


Figure 9. Influence of infiltration on sediment deposition at different slopes using sand at a feed rate of 100 g s⁻¹, water inflow at 58 L min⁻¹, and rainfall at 170 mm h⁻¹ (experiment group D).

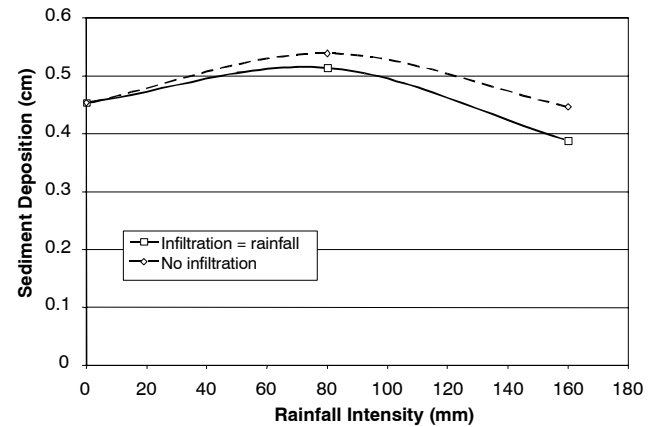


Figure 10. Sediment deposition of experiments F and G with glass beads in an unsaturated (infiltrating) vs. a saturated (non-infiltrating) bed with sediment feed rate of 30 g s⁻¹ and 45 L min⁻¹ flow rate.

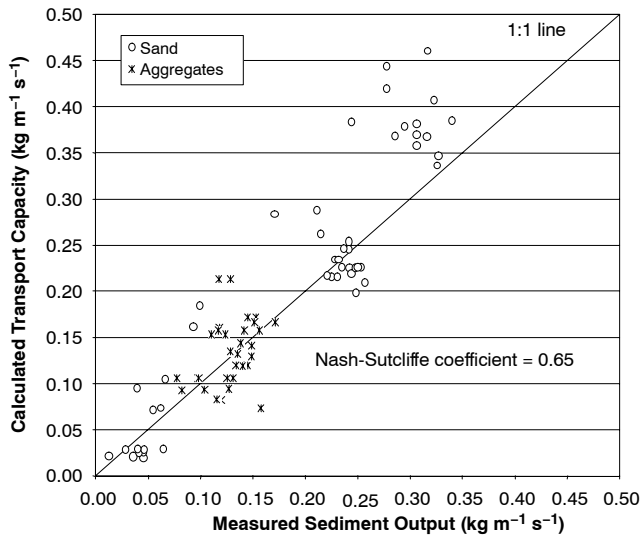


Figure 11. Comparisons of calculated sediment transport capacity with measured sediment output for experiments with sand and plastic/glass aggregates.

with lesser sediment input (experiment group H in table 1), sediment output results were less than the calculated sediment transport capacity, implying that those experiments were in a detachment regime instead of a depositional or equilibrium mode. This was also confirmed by the laser scan results, as shown in figure 7, where the deposition was below 0.

Average values of calculated transport capacities for experiments with 0, 80, and 160 mm h⁻¹ rainfall intensities under unsaturated conditions were compared with measured values for sand, glass beads, and plastic/glass aggregates (table 4). The standard error (SE) and coefficient of variation (CV) was computed between the calculated T_c and measured

sediment output (G_{out}). The SE was calculated as the square root of the average square of differences between T_c and G_{out} , and the CV was calculated by dividing the SE by the average value of G_{out} . Lower values of CV represent a better fit between T_c and G_{out} , as was the case for the sand and plastic/glass aggregates. Differences in CV can also be attributed to interactions between rainfall and flows rates that increase or diminish the CV between T_c and G_{out} . For experiments F and G with glass beads, the calculated transport capacity was less than the measured sediment output. This implies that the Yalin equation underpredicted the transport capacity for this sediment type. The glass beads' unique physical properties, such as their nearly perfect spherical shape (fig. 2) and higher measured than calculated fall velocity (table 2), may have contributed to underprediction of transport capacity with the Yalin equation.

Modeling of deposition was done to quantify the β turbulence factor based on the interactions of rainfall intensity with water flow depth. The calculation of the β factor is also dependent on the estimation of transport capacity. If transport capacity is above the sediment input (G_{in}), then the system is considered to be in a detachment regime, which requires the use of a different set of equations, and β can no longer be calculated. Therefore, all experiments where calculated transport capacity was greater than sediment input (G_{in}) were excluded from the analyses. This mainly excluded experiments with the artificial aggregates with low sediment feed rate (experiment group H), which were in a detachment regime. A negative β value would reflect conditions in which either G_{out} was greater than G_{in} or T_c was greater than G_{in} , which can occur when T_c is overestimated.

Since the β value was dependent on T_c , alternate β values were evaluated using three different transport capacity

Table 4. Calculation of transport capacity (T_c) and comparison to measured sediment output.

Sediment Type (Experiment Group)	Reps	Rainfall (mm h ⁻¹)	Target Flow Rate (L min ⁻¹)	Sediment Input G_{in} (kg m ⁻¹ s ⁻¹)	Average Calculated T_c (kg m ⁻¹ s ⁻¹)	Average G_{out} ^[a] (kg m ⁻¹ s ⁻¹)	Average $G_{in} - G_{out}$ ^[a] (kg m ⁻¹ s ⁻¹)	SE ^[b]	CV ^[b]
								between G_{out} and T_c	between G_{out} and T_c
Sand (E)	5	0	45	0.415	0.216	0.247	0.167	0.035	0.139
	5	80	45	0.415	0.232	0.233	0.181	0.010	0.042
	3	160	45	0.415	0.232	0.236	0.178	0.014	0.059
	4	0	60	0.415	0.374	0.310	0.105	0.071	0.229
	3	80	60	0.415	0.382	0.299	0.115	0.097	0.323
	3	160	60	0.415	0.365	0.309	0.105	0.056	0.182
Glass Beads (F)	3	0	45	0.139	0.045	0.106	0.033	0.062	0.587
	4	80	45	0.139	0.056	0.104	0.035	0.050	0.479
	3	160	45	0.139	0.062	0.084	0.055	0.038	0.452
	3	0	45	0.198	0.039	0.173	0.025	0.135	0.781
	2	80	45	0.198	0.051	0.161	0.037	0.112	0.698
	2	160	45	0.198	0.066	0.149	0.049	0.098	0.654
	3	0	45	0.415	0.030	0.253	0.162	0.227	0.895
	4	80	45	0.415	0.036	0.199	0.216	0.166	0.834
2	160	45	0.415	0.035	0.184	0.230	0.159	0.862	
Aggregates (I)	5	0	20	0.154	0.108	0.122	0.032	0.023	0.189
	6	80	20	0.154	0.094	0.105	0.049	0.040	0.379
	4	160	20	0.154	0.110	0.127	0.027	0.018	0.140
	6	0	30	0.154	0.155	0.139	0.015	0.023	0.167
	6	80	30	0.154	0.140	0.134	0.020	0.028	0.207
	6	160	30	0.154	0.183	0.141	0.013	0.055	0.388

[a] G_{out} = measured sediment output, and $G_{in} - G_{out}$ = sediment accumulated.

[b] SE = standard error, and CV = coefficient of variation.

Table 5. Calculation of average β values by using three methods of defining the transport capacity (T_c).

Sediment Type (Experiment Group)	Rainfall (mm h ⁻¹)	Target Flow Rate (L min ⁻¹)	Sediment Input G_{in} (kg m ⁻¹ s ⁻¹)	Actual Average Flow Depth (m)	β ($T_c = G_{out}$)		β (Yalin T_c)		β (fixed T_c)	
					Average	St. Dev.	Average	St. Dev.	Average	St. Dev.
Sand (E)	0	45	0.415	0.0054	0.0156	0.0004	0.0132	0.0012	0.0156	0.0007
	80	45	0.415	0.0056	0.0161	0.0006	0.0161	0.0015	0.0174	0.0005
	160	45	0.415	0.0056	0.0160	0.0000	0.0157	0.0014	0.0171	0.0011
	0	60	0.415	0.0072	0.0215	0.0003	0.1123 ^[a]	0.1219 ^[a]	0.0216	0.0040
	80	60	0.415	0.0073	0.0219	0.0003	0.0520	0.0339	0.0241	0.0054
	160	60	0.415	0.0071	0.0217	0.0004	0.0467	0.0053	0.0219	0.0008
Glass Beads (F)	0	45	0.139	0.0059	0.0451	0.0009	0.0157	0.0055	0.0170	0.0056
	80	45	0.139	0.0066	0.0496	0.0037	0.0206	0.0080	0.0197	0.0086
	160	45	0.139	0.0070	0.0505	0.0024	0.0380	0.0273	0.0326	0.0205
	0	45	0.198	0.0056	0.0427	0.0005	0.0070	0.0056	0.0164	0.0127
	80	45	0.198	0.0063	0.0451	0.0051	0.0123	0.0070	0.0259	0.0109
	160	45	0.198	0.0071	0.0478	0.0089	0.0222	0.0210	0.0370	0.0266
	0	45	0.415	0.0049	0.0412	0.0005	0.0173	0.0049	0.0156	0.0043
	80	45	0.415	0.0053	0.0430	0.0023	0.0247	0.0048	0.0219	0.0041
	160	45	0.415	0.0053	0.0415	0.0000	0.0252	0.0082	0.0224	0.0071
	Aggregates (I)	0	20	0.154	0.0066	0.0042	0.0002	0.0032	0.0024	0.0074
80		20	0.154	0.0063	0.0038	0.0001	0.0035	0.0017	0.0110	0.0043
160		20	0.154	0.0066	0.0040	0.0001	0.0019	0.0012	0.0056	0.0048
0		30	0.154	0.0076	0.0054	0.0004	-0.0068 ^[b]	0.0151	0.0092	0.0182
80		30	0.154	0.0073	0.0051	0.0002	-0.0016 ^[b]	0.0105	0.0152	0.0124
160		30	0.154	0.0082	0.0054	0.0001	0.0002	0.0024	0.0070	0.0171

^[a] High β and standard deviation due to high estimation of one T_c value.

^[b] Negative β values show situations in which some of the individual experimental repetitions showed either higher T_c values than G_{in} or higher G_{out} than G_{in} .

determinations: (1) T_c was assumed to be equal to the sediment output from the end of the rill and is represented by β ($T_c = G_{out}$); (2) T_c was calculated using the Yalin equation and is represented by β (Yalin T_c); and (3) T_c was fixed for individual sets of rainfall experiments using the T_c determined from the no-rainfall experiments and is represented by β (fixed T_c). The β values were well below the fixed 0.5 value used in WEPP for all three procedures for estimating T_c (table 5).

The β (Yalin T_c) values for sand ranged from 0.0132 to 0.0520 with one outlier at 0.1123, glass beads were between 0.0070 and 0.0382, and aggregates were between 0.0002 and 0.0035 with two negative values caused by high Yalin T_c computations (table 5). Mean β (Yalin T_c) values calculated with no rainfall were in general lower than values calculated with rainfall; however, some values are compensating for limitations in the calculation of T_c . The β ($T_c = G_{out}$) has a mixed relationship with rainfall intensities but a distinct relationship with sediment type. Values of β ($T_c = G_{out}$) for sand ranged from 0.0156 to 0.0219, whereas values for glass beads ranged from 0.0412 to 0.0505 and values for aggregates ranged from 0.0042 to 0.0054. The β (fixed T_c) calculated for 80 mm h⁻¹ rainfall intensity had a greater average value than β (fixed T_c) calculated for 0 and 160 mm h⁻¹ rainfall intensities for sand and aggregates. For glass beads, the value of β (fixed T_c) increased with an increase in rainfall intensity. The results of all β calculations indicated that β was dependent on the sediment type, with aggregates having lower β values than sand or glass beads. The results also showed that β was related to flow depth (table 5); therefore, it was important to determine how flow depth interacted with rainfall intensity for the calculation of β .

A multiple regression model to estimate the β factor was developed relating β to the flow depth and rainfall intensity.

The multiple regressions helped determine the relative importance of rainfall intensity and flow depth for estimating β . Multiple regressions were conducted separately for the sand, glass beads, and aggregates because of the differences in particle densities, sizes, and shapes that have an effect on their transport capacity. As expected, the β values calculated by setting the transport capacity equal to the output sediment provided the best fit as indicated by greater adjusted R² values for all sediment types, as well as from the lesser standard errors (table 6).

In table 7, the actual coefficients of the multiple regressions are reported (where $\beta = \text{Coef1}^*(\text{rainfall intensity}) + \text{Coef2}^*(\text{flow depth})$). Table 7 also shows the importance of each factor (rainfall or flow depth) through the t-statistic and P-value. When the P-value is closer to 0, the factor was more significant, and therefore flow depth was the most important factor overall (table 7). When calculating β ($T_c =$

Table 6. Comparison of the three methods to calculate β by using a multiple regression analysis in which β is estimated based on rainfall intensity and flow depth.

Sediment Type	Statistic	β ($T_c = G_{out}$)	β (Yalin T_c)	β (fixed T_c)
Sand	Adjusted R ²	0.95	0.37	0.94
	Standard error	0.00064	0.05532	0.00200
	Observations	22	22	22
Glass Beads	Adjusted R ²	0.95	0.75	0.83
	Standard error	0.00403	0.01104	0.00926
	Observations	26	26	26
Aggregates	Adjusted R ²	0.95	0.00 ^[a]	0.61
	Standard error	0.00033	0.00927	0.01162
	Observations	25	25	25

^[a] Value is less than 0.001.

Table 7. Coefficients and statistical significance of rainfall intensity and flow depth in estimating β using a multiple regression approach (eq. 7).

Independent Factors	Dependent Factor β	Sediment Type	Rainfall or Flow Depth Coefficients	Standard Error	t-Statistic	P-Value
Rainfall	$\beta (T_c = G_{out})$	Sand	1.76E-07	2.10E-06	0.0840	0.9339
		Glass Beads	-1.38E-05	1.35E-05	-1.0228	0.3166
		Aggregates	-2.36E-06	1.04E-06	-2.2669	0.0331
	$\beta (Yalin T_c)$	Sand	-2.49E-04	1.81E-04	-1.3769	0.1838
		Glass Beads	8.13E-05	3.71E-05	2.1920	0.0383
		Aggregates	3.67E-05	2.97E-05	1.2368	0.2286
	$\beta (fixed T_c)$	Sand	4.83E-06	6.54E-06	0.7377	0.4693
		Glass Beads	5.95E-05	3.11E-05	1.9134	0.0677
		Aggregates	-2.88E-05	3.72E-05	-0.7730	0.4474
Flow depth	$\beta (T_c = G_{out})$	Sand	2.9736	0.0321	92.6248	8.168E-28
		Glass Beads	7.6681	0.2165	35.4208	3.109E-22
		Aggregates	0.6661	0.0143	46.5680	2.882E-24
	$\beta (Yalin T_c)$	Sand	9.9767	2.7654	3.6077	1.757E-03
		Glass Beads	2.4811	0.5935	4.1803	3.338E-04
		Aggregates	-0.5295	0.4069	-1.3014	2.060E-01
	$\beta (fixed T_c)$	Sand	2.9893	0.1001	29.8700	4.568E-18
		Glass Beads	3.1006	0.4977	6.2301	1.940E-06
		Aggregates	2.5097	0.5102	4.9191	5.701E-05

G_{out}), the importance of rainfall intensity was only evident for the aggregates (where the P value is 0.0331). When calculating β (Yalin T_c), glass beads appeared to have rainfall as an important factor in computing β . This may be, however, because β was being used to compensate for the limitations of the calculation of T_c with the Yalin equation for glass beads. A similar overcompensation happened for β (fixed T_c); therefore, it was believed that an equation using $\beta (T_c = G_{out})$ best represented the influence of rainfall and flow depth induced turbulence. This equation for sand at 5% slope was:

$$\beta = R \cdot 1.76 \cdot 10^{-7} + F \cdot 2.97 \quad (7)$$

where R is the rainfall intensity (mm h^{-1}), and F is the water flow depth (m).

A test to appreciate the applicability of this equation for sand at 5% slope is presented in table 8. The data used in this example were not used in the original determination of β and are therefore independent. Table 8 shows a comparison of using equation 7 for calculating β as compared to the standard practice of using 0 for equilibrium conditions ($G_{in} = G_{out}$), 0.5 for shallow flows, and 1 for other conditions. The results show that the G_{out} calculated with the equation of $\beta (T_c = G_{out})$ matched closely the measured value as compared to using the fixed values of 0, 0.5, and 1. Although the table only shows a limited example using sand, a similar improvement of estimation of deposition in rills under rainfall and shallow

flows can be made using lesser density and finer-sized soil particles, as the experiments with aggregates show. Furthermore, if a fixed value is to be used for β when simulating deposition of non-cohesive sediment under shallow flows in a rill, the value should probably be less than the 0.5 currently used, as all these experiments showed.

SUMMARY AND CONCLUSIONS

Laboratory experiments were conducted to study the influence of rainfall intensity and flow depth on deposition of non-cohesive soil in a rill. Results showed that deposition as affected by both rainfall intensity and flow depth was dependent on the particle type and its physical properties. For example, deposition of sand with specific gravity of 2.65 was not significantly affected by different rainfall intensities for the flows and slopes tested. However, a significant effect of rainfall intensity on deposition was seen in the experiments carried out using less-dense plastic/glass aggregates and fine-sized glass beads in a high-deposition regime. Experiments with glass beads and aggregates under greater interrill contributions showed that deposition was greater with the 80 mm h^{-1} rainfall and was less with the 0 and 160 mm h^{-1} rainfalls. Increased turbulence from the 160 mm h^{-1} rainfalls can explain the reduced deposition rates at the greater rainfall intensity. During no rainfall, water flow was not evenly

Table 8. Examples of the comparison of measured and calculated sediment output (G_{out}) for sands in a saturated rill with 5% slope under rainfall using the β equation, $\beta = 0$, $\beta = 0.5$, and $\beta = 1$.

Rainfall (mm h^{-1})	Flow Depth (m)	Calculated T_c ($\text{kg m}^{-1} \text{s}^{-1}$)	β Equation	G_{out} ($\text{kg m}^{-1} \text{s}^{-1}$)				
				Measured	β Equation	$\beta = 0^{[a]}$	$\beta = 0.5$	$\beta = 1$
80	0.0059	0.262	0.018	0.214	0.250	0.415	-4.230	-8.874
80	0.0055	0.227	0.016	0.253	0.223	0.415	-5.442	-11.299
80	0.0080	0.461	0.024	0.317	0.460	0.415	1.367	2.320
160	0.0058	0.247	0.017	0.236	0.246	0.415	-4.500	-9.415
160	0.0073	0.386	0.022	0.340	0.388	0.415	-0.194	-0.803

[a] Represents a situation where there is no deposition, where $G_{in} = G_{out}$.

distributed on the surface of the rill, causing meandering and concentrated flows, which may have caused increased scouring and therefore less deposition. Results show that low or medium rainfall intensities may have the positive effect of reducing erosion in rills when compared to either no rainfall or high-intensity rainfall. However, further experiments are needed to determine if the peak effect is at 80 mm h⁻¹ or at lower intensities, and to show how this effect is related to other properties such as flow depth, sediment type, slope, and interrill contribution.

A set of experiments conducted to study the influence of infiltration on deposition under rainfall showed that at slopes less than 3% there was more deposition when the rill was in a saturated stage than in an unsaturated or active infiltration stage. At slopes greater than 3%, the opposite was true. Active infiltration may cause a suction effect on flows and sediment, inducing deposition. However, active infiltration also meant that flows had slightly less water than saturated conditions because part of this water was being infiltrated. It is therefore possible that at lower slopes in the saturated stage, slightly greater flow depths and therefore less turbulence induced by rainfall led to greater deposition. At steeper slopes under saturated conditions, greater detachment occurred because the flow depth may have been sufficiently shallow to allow rainfall to cause more turbulence. More research is needed to establish relationships between sediment deposition and slope, particle type, flows, and infiltration.

Modeling deposition using the WEPP equations showed that a β turbulence factor equal to 0.5, as used in the WEPP model for flow in a rill with the influence of rainfall, did not adequately predict the deposition on the bed for these experiments using non-cohesive sediment. Calculated β values for experiments using the measured sediment transport capacity ($T_c = G_{out}$) ranged from 0.0156 to 0.0219 for sands, from 0.0412 to 0.0505 for glass beads, and from 0.0042 to 0.0054 for the larger but less dense plastic/glass aggregates. However, β values calculated using the Yalin estimated T_c for the same experiments ranged from 0.0132 to 0.0520 for sands, from 0.0070 to 0.0380 for glass beads, and lower than 0.0035 for the aggregates. These results show the dependency of β on T_c ; therefore, it is recommended that further review of the WEPP equations be made, with consideration that lesser β values may be more appropriate for non-cohesive soils than the default value of 0.5 currently used, at least for the range of flow depths observed in these experiments. Lowering the β value in the WEPP equation would reduce deposition rates and potentially increase sediment transported through a rill that is in a depositional mode. This would not have direct implications on detachment rates but only on where the sediment is deposited.

Alternatively, other transport capacity equations should be examined and adjusted to predict deposition in conditions of shallow and turbulent flow for sands and for particles of different densities. Changing the transport capacity would have implications on detachment as well as deposition. Further experiments with smaller particles of different densities and different flow conditions should be performed in order to establish a more global function that relates β to rainfall intensity, sediment type, and flow depth.

REFERENCES

- Alonso, C. V., W. H. Neibling, and G. R. Foster. 1981. Estimating sediment transport capacity in watershed modeling. *Trans. ASAE* 24(5): 1211-1220, 1226.
- Beuselinck, L., G. Govers, A. Steegen, and T. A. Quine. 1999. Sediment transport by overland flow over an area of net deposition. *Hydrological Processes* 13(17): 2769-2782.
- Beuselinck, L., G. Govers, P. B. Hairsine, G. C. Sander, and M. Breynaert. 2002. The influence of rainfall on sediment transport by overland flow over areas of net deposition. *J. Hydrology* 257(2002): 145-163.
- Cochrane, T. A., and D. C. Flanagan. 1997. Detachment in a simulated rill. *Trans. ASAE* 40(1): 111-119.
- Flanagan, D. C., and M. A. Nearing, eds. 1995. *USDA - Water Erosion Prediction Project: Hillslope Profile and Watershed Model Documentation*. NSERL Report No. 10. West Lafayette, Ind.: USDA-ARS National Soil Erosion Research Laboratory.
- Flanagan, D. C., C. Huang, L. D. Norton, and S. C. Parker. 1995. Laser scanner for erosion plot measurements. *Trans. ASAE* 38(3): 703-710.
- Foster, G. R. 1982. Modeling the erosion process. In *Hydrologic Modeling of Small Watersheds*, 328-347. C. T. Haan, H. P. Johnson, and D. L. Brakensiek, eds. ASAE Monograph No. 5. St. Joseph, Mich.: ASAE.
- Foster, G. R., and L. D. Meyer. 1972. Transport of soil particles by shallow flow. *Trans. ASAE* 15(1): 99-102.
- Foster, G. R., W. H. Neibling, and R. A. Natterman. 1982. A programmable rainfall simulator. ASAE Paper No. 822570. St. Joseph, Mich.: ASAE.
- Foster, G. R., D. C. Flanagan, M. A. Nearing, L. J. Lane, L. M. Risse, and S. C. Finkner. 1995. Hillslope erosion component. In *USDA - Water Erosion Prediction Project: Hillslope Profile and Watershed Model Documentation*. NSERL Report No. 10. D. C. Flanagan and M.A. Nearing, eds. West Lafayette, Ind.: USDA-ARS National Soil Erosion Research Laboratory.
- Hairsine, P., and G. McTainsh. 1986. The Griffith tube: A simple settling tube for the measurement of settling velocity of aggregates. AES Working Paper. Brisbane, Australia: Griffith University, School of Australian Environmental Studies.
- Kinnell, P. I. A. 1988. The influence of flow discharge on sediment concentrations in raindrop-induced flow transport. *Australian J. Soil Res.* 26(4): 575-581.
- Kinnell, P. I. A. 1991. The effect of flow depth on sediment transport induced by raindrops impacting shallow flows. *Trans. ASAE* 34(1): 161-168.
- Laursen, E. 1958. The total sediment load of streams. *J. Hydraul. Div. ASCE* 54(HY1): Paper 1530.
- Meyer, L. D., B. A. Zuhdi, N. L. Coleman, and S. N. Prasad. 1983. Transport of sand-sized sediment along crop-row furrows. *Trans. ASAE* 26(1): 106-111.
- Moss, A. J. 1988. Effects of flow-velocity variation on rain-driven transportation and the role of rain impact in the movement of solids. *Australian J. Soil Res.* 26(3): 443-450.
- Moss, A. J., and P. Green. 1983. Movement of solids in air and water by raindrop impact: Effects of drop-size and water-depth variations. *Australian J. Soil Res.* 21(3): 257-269.
- Moss, A. J., P. H. Walker, and J. Hutka. 1979. Raindrop-stimulated transportation in shallow water flows: An experimental study. *Sediment. Geol.* 22(3-4): 165-184.
- Shields, A. 1936. Application of similarity principles and turbulence research to bed-load movement. *Mitteilungen der Preussischen Versuchsanstalt für Wasserbau und Schiffbau* 26: 5-24.
- Schmidt, J. 1991. The impact of rainfall on sediment transport by sheetflow. *Catena Supplement* 19, Cremlingen: 9-17.
- Yalin, M. S. 1963. An expression for bed-load transportation. *J. Hydraul. Div. ASCE* 89(HY3): 221-250.
- Yang, C. T. 1973. Incipient motion and sediment transport. *J. Hydraul. Div. ASCE* 99(HY10): 1679-1704.

